
iSeg: An Iterative Refinement-based Framework for Training-free Segmentation

Lin Sun¹, Jiale Cao¹, Jin Xie³, Fahad Shahbaz Khan², Yanwei Pang^{1,4}

¹ Tianjin University ² Mohamed bin Zayed University of Artificial Intelligence

³ Chongqing University ⁴ Shanghai Artificial Intelligence Laboratory
sun0806@tju.edu.cn connor@tju.edu.cn xiejin@cqu.edu.cn

fahad.khan@mbzuai.ac.ae pyw@tju.edu.cn

Abstract

Stable diffusion has demonstrated strong image synthesis ability to given text descriptions, suggesting it to contain strong semantic clue for grouping objects. Inspired by this, researchers have explored employing stable diffusion for training-free segmentation. Most existing approaches either simply employ cross-attention map or refine it by self-attention map, to generate segmentation masks. We believe that iterative refinement with self-attention map would lead to better results. However, we empirically demonstrate that such a refinement is sub-optimal likely due to the self-attention map containing irrelevant global information which hampers accurately refining cross-attention map with multiple iterations. To address this, we propose an iterative refinement framework for training-free segmentation, named iSeg, having an entropy-reduced self-attention module which utilizes a gradient descent scheme to reduce the entropy of self-attention map, thereby suppressing the weak responses corresponding to irrelevant global information. Leveraging the entropy-reduced self-attention module, our iSeg stably improves refined cross-attention map with iterative refinement. Further, we design a category-enhanced cross-attention module to generate accurate cross-attention map, providing a better initial input for iterative refinement. Extensive experiments across different datasets and diverse segmentation tasks (weakly-supervised semantic segmentation, open-vocabulary semantic segmentation, unsupervised segmentation, and mask generation on synthetic dataset) reveal the merits of proposed contributions, leading to promising performance on diverse segmentation tasks. For unsupervised semantic segmentation on Cityscapes, our iSeg achieves an absolute gain of 3.8% in terms of mIoU compared to the best existing training-free approach in literature. Moreover, our proposed iSeg can support segmentation with different kind of images and interactions. Our project page is publicly released at <https://linsun449.github.io/iSeg/>.

1 Introduction

Semantic segmentation [1–3] aims to differentiate the pixels into different semantic groups. In past decade, fully-supervised semantic segmentation has achieved significant progress where the models are trained on large-scale datasets with pixel-level annotations and fixed categories. This fully-supervised setting hinders zero-shot segmentation ability on unseen categories. Further, it is expensive to collect and annotate large-scale dataset with numerous categories [4] for model training. One straightforward solution is to develop a universal and training-free framework that exhibits strong generalization capabilities across arbitrary categories without any training on segmentation datasets.

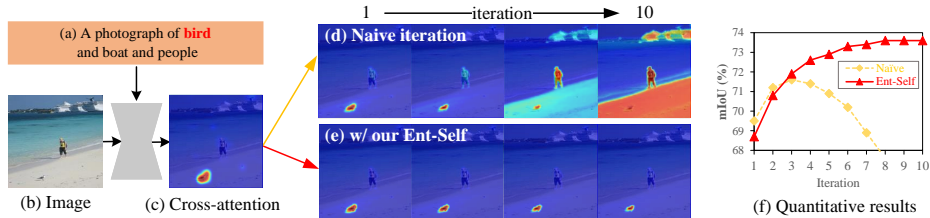


Figure 1: **Comparison of naive iteration strategy and our entropy-reduced self-attention module.** We feed text prompt (a) and image (b) into pre-trained stable diffusion to extract the cross-attention map (c) and self-attention map. Afterwards, we refine the cross-attention map with self-attention map using naive iteration strategy (d) and our entropy-reduced self-attention (Ent-Self) module (e). Compared to naive iteration strategy, our Ent-Self module can generate accurate refined cross-attention map after multiple iterations. In (f), we give the quantitative comparison of naive iteration strategy and our Ent-Self module on pseudo mask generation in weakly-supervised semantic segmentation.

Recent work of [5] introduces a vision-language model, CLIP, that learns the connection between text and images through training on large-scale image-text pairs, showing promising generalization capabilities in recognizing arbitrary categories. Inspired by this, several works [6–9] explore employing the strong zero-shot ability of CLIP for semantic segmentation. Some works focus on directly utilizing the learned text-image mapping from pre-trained CLIP. For instance, OVSeg [6] first utilizes mask proposal generator to extract some class-agnostic masks, and then employs CLIP to classify cropped and masked images for open-vocabulary semantic segmentation. Some works employ text supervision similar to CLIP. For instance, GroupViT [8] introduces a hierarchical grouping vision transformer with text supervision, which is able to group different semantic regions without pixel-level annotations. These methods improve the generalization ability of semantic segmentation or reduce the reliance on pixel-level annotations in some degree. However, CLIP focuses on image-level information, limiting its capability in pixel-level tasks, especially under training-free setting.

Recently, researchers started to employ text-to-image stable diffusion model for segmentation. Stable diffusion [10] was initially designed to perform high-quality image synthesis. With the pre-training on large-scale text-image paired data, stable diffusion is able to generate high-quality images with reasonable structure according to given text descriptions. Inspired by this, researchers believed that stable diffusion contains rich semantic clue to group objects, and proposed various diffusion-based segmentation approaches. Some approaches [11–14] treat stable diffusion as feature extractor, and re-train it on segmentation dataset. In contrast, other approaches [15–17] explore training-free framework by utilizing self-attention map and cross-attention map in stable diffusion. For instance, DiffSeg [15] iteratively merges self-attention maps at different positions and employs non-maximum suppression to assign the pixels into different objects. DiffuMask [18] generates initial object masks of synthetic images using cross-attention maps. DiffSegmenter [16] refines the cross-attention map with self-attention map for improved segmentation. These approaches present an initial attempt on employing self-attention and cross-attention maps for training-free segmentation tasks. However, we argue that it is still an open problem about how to fully harness self-attention and cross-attention maps for segmentation tasks.

To fully exploit the potential ability of cross-attention and self-attention maps in stable diffusion for training-free segmentation, we conduct a preliminary experiment, where we iteratively refine the cross-attention map with self-attention map as in Fig. 1. Given a text prompt (a) and an image (b), we employ stable diffusion to extract cross-attention map (c) of category bird. Subsequently, we perform a naive iteration strategy to refine the cross-attention map by iteratively multiplying self-attention map. After several iterations, we observe that the refined cross-attention map associated with category bird gradually has strong response on other regions, such as person and sandwich in (d). We argue that this degradation in refined cross-attention map is caused by self-attention map that aggregates global information from irrelevant regions after multiple iterations. To address this issue, we propose an iterative refinement framework by introducing an entropy-reduced self-attention (Ent-Self) module to impede the information aggregation from irrelevant regions. As in (e), our Ent-Self module is able to generate a stable and accurate cross-attention map of bird after multiple iterations. We further give a quantitative comparison of generated pseudo mask for weakly-supervised semantic segmentation in (f). Compared to naive iteration strategy, our Ent-Self module exhibits improved performance with the increment of iterations. In addition, we design a simple category-enhanced cross-attention (Cat-Cross) module to generate more accurate cross-attention map as the input fed to iterative refinement. The

Cat-Cross module employs a weighting strategy to enhance the text embeddings of given category while suppressing other words. We perform the experiments on various datasets and segmentation tasks, which demonstrate method efficacy.

2 Related works

Semantic segmentation. Initially, researchers mainly investigated CNN-based networks. One of the pioneering approaches is FCN [19], which utilizes convolutional neural networks with skip-layer connections. Subsequently, numerous variants were developed, incorporating innovations such as spatial pyramid structures [1, 20], multi-layer feature fusion [21–23], and non-local enhancements [24–26]. With the success of vision transformer in image classification [27, 28], researchers began to explore transformer-based approaches. Some studies [29, 30, 3] focus on harnessing the powerful representational capabilities of transformer by employing it as backbone. Additionally, other researches [31, 32] conceptualize semantic segmentation as a set prediction task, utilizing the transformer as decoder.

Besides, researchers developed various semantic segmentation paradigms. Weakly-supervised semantic segmentation [33–35] solely relies on image-level category annotations to train models. For this task, many researchers employed CAM [36] to generate pseudo pixel-level annotations and then trained models with these annotations. Open-vocabulary semantic segmentation [37, 38, 8] performs semantic segmentation on unseen categories. In open-vocabulary semantic segmentation, researchers mainly explored to utilize CLIP [5] to segment unseen categories. Unsupervised segmentation [39–41] aims to group the pixels belonging to the same objects without using any annotations.

Diffusion models for segmentation. Diffusion models [42] have exhibited strong image synthesis ability across various text prompts, indicating their strong semantic clue for image segmentation. Inspired by this, researchers started to employ the pre-trained diffusion models for segmentation. For instance, VPD [13] views stable diffusion model as feature extractor, and fine-tunes them for semantic segmentation tasks. TADP [43] introduces image-aligned text prompts to condition diffusion model for segmentation. SLIME [44] adopts stable diffusion model with learnable text embeddings for few-shot segmentation. Additionally, some researchers [45] adopted diffusion framework for predicting accurate segmentation maps from noisy data.

Recently, some researchers explored training-free diffusion models for segmentation. One of the key idea is to employ self-attention map and cross-attention map from pre-trained diffusion model to generate masks of semantic categories. For instance, DiffuMask [18] first employs diffusion model to generate synthetic images, and calculates the averaged cross-attention map as the initial object masks. DiffSeg [15] explores grouping self-attention maps at different positions into distinct objects based on their similarities, followed by non-maximum suppression to assign pixels to individual objects. OVDiff [46] generates synthetic images by diffusion model, and uses a feature extractor to generate the foreground and background prototypes of different categories for open-vocabulary segmentation. Both Diffsegmenter [16] and T2M [17] refine cross-attention maps of different categories with self-attention maps. To improve cross-attention map, Diffsegmentor and T2M employ additional BLIP [47] and CLIP to carefully design text prompts, which are relatively complex in some degree. Though these aforementioned approaches exploit self-attention and cross-attention maps for training-free segmentation, we argue that these approaches do not fully utilize the semantic clue existing in self-attention and cross-attention maps. To address this issue, we propose an iterative training-free segmentation framework using pre-trained stable diffusion model.

3 Method

3.1 Preliminaries

Stable diffusion model. Text-to-image (T2I) diffusion model is a type of text-conditioned diffusion models [42], such as DALL-E [48], GLIDE [49], Imagen [50], and stable diffusion [10]. As one of representative T2I models, stable diffusion generates high-quality images with text prompts, which is trained on large-scale text-image paired dataset (*e.g.*, LAION-5B [51]). It comprises three components: (1) A pre-trained VAE [52] encoder and decoder for image compression and restoration. (2) A text encoder that encodes text descriptions into latent semantic space. (3) A transformer-based denoising UNet [53] that recovers images from noisy data according to text descriptions.

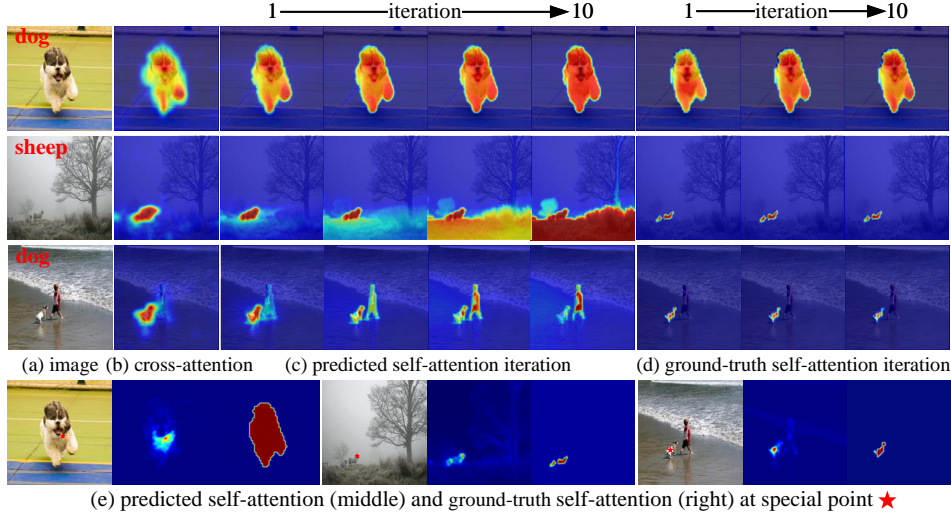


Figure 2: **Cross-attention map refinement with predicted self-attention map and ground-truth self-attention map.** Given the image (a) and cross-attention map (b), we first give the refined cross-attention maps at different iterations using predicted self-attention map in (c). At the same time, we present the refined cross-attention maps using ground-truth self-attention map in (d), where ground-truth self-attention map is generated by ground-truth masks. Finally, we compare the predicted self-attention map and ground-truth self-attention map in (e), where predicted self-attention map is noisy and ground-truth self-attention map is clean.

Attention modules. Denoising UNet in stable diffusion integrates self-attention and cross-attention mechanisms. The self-attention models the relation between different spatial positions of visual features, while the cross-attention models the relation between visual features and text embeddings. The attention map in both self-attention and cross-attention operations can be calculated by the query Q and the key V as $A = \text{Softmax}(QK^T/\sqrt{d})$, where d is normalization factor. Assuming that the visual features has the spatial size of $H \times W$, and the text embeddings has the length of T . In self-attention operation, the query and key are both generated by visual features via linear layers. The generated self-attention map is denoted as $A_{sa} \in \mathcal{R}^{HW \times HW}$, which can reflect spatial similarities of different positions within image. In cross-attention operation, the query and key are respectively generated by visual features and text embeddings via linear layers. The generated cross-attention map is denoted as $A_{ca} \in \mathcal{R}^{HW \times T}$, capturing the similarities between image and text.

To achieve training-free segmentation, a straightforward way is setting the text prompts based on given category names, such as ‘A photograph of cat and dog’, then performing the forward process of stable diffusion and finally generating the corresponding cross-attention map A_{ca} between visual features and text embeddings. Afterwards, we can predict segmentation map based on the obtained cross-attention map associated with corresponding category name. Instead of directly using cross-attention map, some researchers [44] proposed to generate refined cross-attention map A_{ca}^1 with self-attention map, which can be written as

$$A_{ca}^1 = A_{sa} \times A_{ca}. \quad (1)$$

Compared to original cross-attention map, the refined cross-attention map incorporates spatial similarities between different positions existing in self-attention map [44], which is useful to perform accurate segmentation.

3.2 Motivation

Problem. As mentioned above, self-attention map can be used to refine the cross-attention map. Therefore, a natural question is that, can we improve cross-attention map iteratively with self-attention map, formulated as $A_{ca}^n = A_{sa} \times A_{ca}^{n-1}$, where n is the index of iterations. We initially believe that this iterative refinement would yield improved segmentation performance. However, as in Fig. 1(f), it presents performance degradation after several iterations. To better analyze this question, we perform the experiment in Fig. 2. Given the input image (a) and cross-attention map (b), we present the refined cross-attention map at different iterations in (c). It can be observed that the refinement through

multiple iterations can not guarantee to generate better refined cross-attention map. We divide the refined results into three situations. The first situation is that the cross-attention map becomes better with the increasing iterations, such as cross-attention map of dog in first row. The second one is the cross-attention map becomes larger, such as the cross-attention map of sheep in the second row. The last one is that the cross-attention map shifts to other regions, exemplified by the cross-attention map of dog showing strong response on the person in third row.

Analysis. Ideally, we argue the refinement with multiple iterations at least presents a stable cross-attention map around corresponding category if the self-attention map is relatively accurate. We further perform a simple experiment by refining cross-attention map with ground-truth self-attention map in Fig. 2(d). The ground-truth self-attention map is generated by self-correlation of ground-truth masks, which is binary and exclusively has responses within object regions. By using ground-truth self-attention map, the refined cross-attention map becomes stable and accurate after only one iteration. This observation demonstrates that an accurate self-attention map is crucial for accurately refining cross-attention map. As shown in (e), we compare the predicted self-attention map (middle) and ground-truth self-attention map (right) at a given point \star . Compared to ground-truth self-attention map, predicted self-attention map is relatively noisy and has some weak responses at irrelevant regions. As a result, the refinement with predicted self-attention map aggregates irrelevant global information into the refined cross-attention map. Therefore, we argue that it is important to reduce irrelevant global information within self-attention map for iterative refinement.

3.3 Our iterative refinement framework

Here we introduce our proposed iterative refinement framework for training-free segmentation, named iSeg. We employ pre-trained stable diffusion model for feature extraction, and perform segmentation using the generated self-attention and cross-attention maps with iterative refinement. To address performance degradation issue in iterative refinement, we introduce an entropy-reduced self-attention (Ent-Self) module to suppress irrelevant global information within self-attention map. In addition, we design a category-enhanced cross-attention (Cat-Cross) module to generate more accurate cross-attention map as the input of iterative refinement. The algorithm is detailed in Appendix A.

Iterative refinement. Fig. 3 shows the overall architecture of our proposed iSeg. Given an image I , we feed it into a VAE encoder to extract visual latent features z . At the same time, we employ a text encoder to generate text embeddings ε from corresponding input texts. Afterwards, we feed the visual latent features and text embeddings into the denoising UNet, which is formulated as

$$n_p = \mu(z, \varepsilon, t), \quad (2)$$

where μ represents the denoising U-net, and t indicates the timestep that is set as a fixed value 100 like [16]. Then, we can extract self-attention and cross-attention maps at different layers of denoising UNet. Similar to [44], we only select the high-resolution self-attention map at last decoder layer, and upsample and fuse the cross-attention maps at different decoder layers as initial cross-attention map A_{ca} . For self-attention map A_{sa} , we introduce an entropy-reduced self-attention (Ent-Self) module to reduce irrelevant global information within original self-attention map, where the entropy-reduced self-attention map is represent as A_{sa}^{ent} . Then, we perform the iterative refinement using entropy-reduced self-attention map as

$$A_{ca}^n = A_{sa}^{\text{ent}} * A_{ca}^{n-1}, n = 1, \dots, N \quad (3)$$

where N represents the total number of iterations, and A_{ca}^0 is the original cross-attention map A_{ca} . After each iteration, we add a normalization operation. For simplicity, we do not show the normalization in Eq. 3 and Fig. 3. Finally, we can extract the segmentation map of a category at the index i of text prompts as $M_i = A_{ca}^N[:, i]$. It is worth noting that an accurate initial cross-attention map is also important, which provides a better input for iterative refinement. Therefore, instead of original cross-attention map, we design a simple category-enhanced cross-attention (Cat-Cross) module to obtain more accurate cross-attention map fed to iterative refinement.

Entropy-reduced self-attention module. As mentioned above, the weak responses of irrelevant regions within self-attention map contain the global information and interfere with the refined cross-attention map. To address this issue, we introduce an entropy-reduced self-attention (Ent-Self) module. Following [54], we calculate self-attention entropy by viewing the attention distribution as a

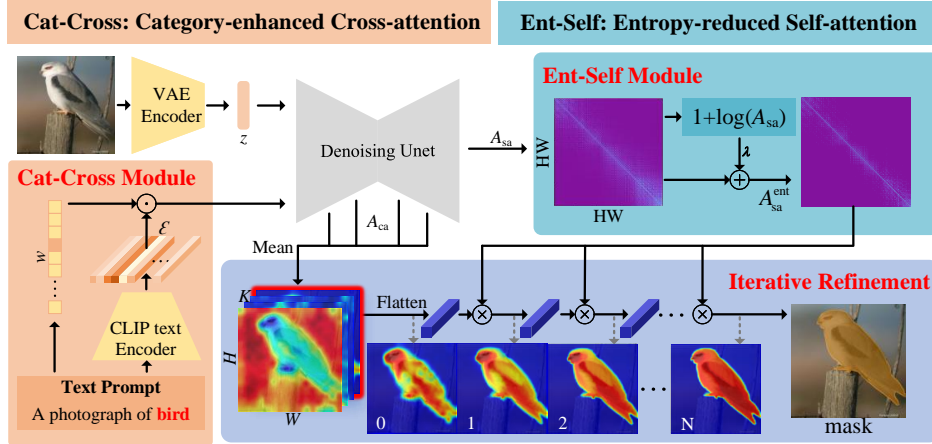


Figure 3: **Architecture of our proposed training-free iSeg.** iSeg comprises two novel modules. The Cat-Cross module generates more accurate cross-attention map, while the Ent-Self module removes the redundant information in self attention map. Given an image with paired text prompt, we first get latent feature z and embedding ε by VAE encoder and Cat-Cross module respectively. These features are fed into denoising U-net to extract cross-attention map A_{ca} and self-attention map A_{sa} . Then the Ent-Self module is applied to reduce entropy of A_{sa} and obtained A_{sa}^{ent} . Finally, an iterative refinement is conducted to refine cross-attention map with entropy-reduced self-attention map.

probability mass function of a discrete random variable, which can be written as

$$E = - \sum_{i=1}^{HW} \sum_{j=1}^{HW} A_{sa}[i, j] \log(A_{sa}[i, j]). \quad (4)$$

The self-attention entropy E has the maximum value when $A_{sa}[i, j] = \frac{1}{N}$ for all elements, and has the minimum value when A_{sa} is binary like ground-truth self-attention map mentioned above. This means that the higher the self-attention entropy is, the more global information will be, and thereby the more likely irrelevant information will be. To reduce the irrelevant information, for a given element A_{sa}^{ij} in self-attention map, the entropy gradient can be calculated as

$$\frac{dE}{dA_{sa}^{ij}} = -(1 + \log(A_{sa}^{ij})). \quad (5)$$

Finally, we calculate the entropy-reduced self-attention map by updating the original self-attention map along negative gradient direction as

$$A_{sa}^{ij} = A_{sa}^{ij} + \lambda(1 + \log(A_{sa}^{ij})), \quad (6)$$

where λ represents the updating factor. The entropy-reduced operation makes the value of A_{sa}^{ij} near to one becomes larger, and makes the value of A_{sa}^{ij} near to zero becomes smaller. As a result, the entropy-reduced operation can suppress the weak responses within self-attention map corresponding to irrelevant global information, and does not reduce the strong responses corresponding to the local region.

Category-enhanced cross-attention module. The accurate cross-attention map presents a good initial state for iterative refinement. Ideally, if we have a perfect cross-attention map, we do not require self-attention refinement. As show in Fig. 4(b), the original cross-attention maps usually have the strong responses on irrelevant regions, such as other categories or background. To improve the quality of cross-attention map fed to the refinement, we introduce a simple category-enhanced cross-attention (Cat-Cross) module, which makes the attention focus more on the text features belonging to the given categories by a factor of γ . Specifically, for a set of given categories

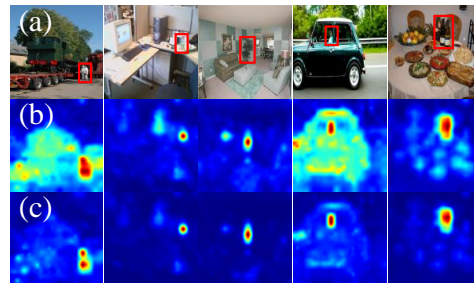


Figure 4: **Compare cross-attention maps** before (b) and after (c) Cat-Cross module.

Table 1: **Comparison of pseudo mask generation with weakly-supervised semantic segmentation approaches.** We report the mIoU results on PASCAL VOC 2012 and MS COCO training sets. Our proposed method outperforms various training-based and training-free approaches.

	Method	Publication	Training	VOC	COCO
CNN-based	IRN [55]	CVPR2019	✓	66.5	42.4
	AdvCAM [56]	CVPR2021	✓	55.6	35.8
	BAS [57]	IJCV2023	✓	57.7	36.9
	HSC [58]	IJCAI2023	✓	71.8	-
Transformer-based	MCTformer [59]	CVPR2022	✓	61.7	-
	MCTformer+ [60]	arXiv2023	✓	68.8	-
	ToCo [61]	CVPR2023	✓	72.2	-
	WeakTr [62]	arXiv2023	✓	66.2	-
CLIP-based	CLIMS [9]	CVPR2022	✓	56.6	-
	CLIP-ES [7]	CVPR2023	✗	70.8	39.7
Diffusion-based	DiffSegmenter [16]	arXiv2023	✗	70.5	-
	T2M [17]	arXiv2023	✗	72.7	43.7
	baseline (Ours)	-	✗	66.0	39.4
	iSeg (Ours)	-	✗	73.6	44.7

\mathcal{C} for segmentation, we generate a weighting vector $W \in \mathcal{R}^{T \times 1}$ as

$$W[j] = \begin{cases} \gamma, & \text{if } j \in \mathcal{C}, \\ 1, & \text{if } j \notin \mathcal{C}, \end{cases} \quad (7)$$

where γ is larger than 1. With the weighting factor W , we generate weighted cross-attention map as

$$A_{ca} = \text{Softmax}\left(\frac{Q(W \cdot K)^T}{\sqrt{d}}\right), \quad (8)$$

where \cdot means element-wise multiplication, the query Q represents visual features, and the key K represents the text embeddings.

4 Experiments

We perform the experiments on weakly-supervised semantic segmentation, open-vocabulary semantic segmentation, unsupervised segmentation, and mask generation for synthetic dataset. Following the prior works [15, 16], we mainly use pixel accuracy (ACC) and mean intersection over union (mIoU) to evaluate segmentation performance.

Implementation details. We employ the pre-trained stable diffusion V2.1 as the base model, and feed the input images into the pre-trained model for segmentation without any training on segmentation dataset. The input images are resized to 512×512 pixels. All segmentation tasks are evaluated on a single NVIDIA RTX 3090 GPU with 24G memory. During inference, only 5G memory is required when using half precision with a batch size of 1, resulting in an approximate inference time of 0.16 seconds per image. For weakly-supervised semantic segmentation, we evaluate pseudo mask generation and use the categories of corresponding training images to generate text prompts. For open-vocabulary semantic segmentation, we employ pre-trained CLIP to generate text prompts. For unsupervised segmentation and mask generation for synthetic dataset, we employ our entropy-reduced self-attention module to refine the segmentation results of DiffSeg [15] and DiffuMask [18]. Please refer to Appendix B for more implementation details of different segmentation tasks.

4.1 State-of-the-art comparison

Weakly supervised semantic segmentation. Table 1 compares our training-free method iSeg and some weakly-supervised methods, including CNN-based, Transformer-based, CLIP-based, and Diffusion-based approaches, on both PASCAL VOC [68] and MS COCO [69] training sets. Here, we only compare the quality of generated pseudo masks. Our proposed iSeg achieves the mIoU scores of 73.6% and 44.7% on PASCAL VOC and MS COCO, respectively. Compared to diffusion-based training-free DiffSegmenter [16] and T2M [17], our iSeg has 3.1% and 0.9% improvements in terms

Table 2: **Comparison with open-vocabulary segmentation approaches.** We reports the mIoU results on PASCAL VOC 2012 validation set, PASCAL-VOC Context validation set, and MS COCO-Object validation set. Our proposed method achieves the promising performance.

	Method	Publication	Training	VOC	Context	Object
CLIP-based	ReCo [41]	NeurIPS2022	✓	25.1	19.9	15.7
	MaskCLIP [63]	ECCV2022	✓	38.8	23.6	20.6
	SegCLIP [64]	ICML2023	✓	52.6	24.7	26.5
	CLIPpy [65]	ICCV2023	✓	52.2	-	32.0
	ViewCo [66]	ICLR2023	✓	52.4	23.0	23.5
	TagCLIP [67]	AAAI2024	✗	64.8	-	-
Diffusion-based	OVDiff [46]	arXiv2023	✗	67.1	30.1	34.8
	DiffSegmenter [16]	arXiv2023	✗	60.1	27.5	37.9
	baseline (Ours)	-	✗	61.4	26.4	36.1
	iSeg (Ours)	-	✗	66.0	30.6	38.2

of mIoU on PASCAL VOC. Our proposed iSeg also outperforms the training-based approaches. For instance, compared to ToCo [61] and WeakTr [62], our proposed iSeg has 1.4% and 7.4% improvements in terms of mIoU on PASCAL VOC.

Open-vocabulary semantic segmentation. Table 2 compares our proposed method with some open-vocabulary semantic segmentation methods, including CLIP-based and diffusion-based approaches, on PASCAL VOC validation set, PASCAL Context validation set [70], and MS COCO Object validation set. Our proposed iSeg outperforms the training-free DiffSegmenter [16] by an absolute gain of 5.9%, 3.1%, and 0.3% on these three datasets.

Unsupervised segmentation. Table 3 compares our method with some unsupervised segmentation methods on Cityscapes [73] validation set and COCO-Stuff-27 [74] validation set. We employ our iterative refinement as a post-processing, and integrate it into unsupervised DiffSeg [15] to improve segmentation results. Our proposed iSeg can also present stable improvement on both Cityscapes and COCO-Stuff-27. For instance, our iSeg outperforms DiffSeg by a large gain of 2.7% in terms of ACC and 3.8% in terms of mIoU on Cityscapes.

Table 3: **Comparison with some unsupervised semantic segmentation approaches.** We report the results on Cityscapes and COCO-Stuff-27 validation sets. Our iSeg stably outperforms DiffSeg and other approaches on these two datasets.

Method	Training	Cityscapes		COCO-Stuff-27	
		ACC	mIoU	ACC	mIoU
IIC [39]	✓	47.9	6.4	21.8	6.7
MDC [71]	✓	40.7	7.1	32.3	9.8
PICLE [72]	✓	65.5	12.3	48.1	13.8
STEGO [40]	✓	73.2	21.0	56.9	28.2
MaskCLIP [63]	✓	35.9	10.0	32.2	19.6
RoCo [41]	✓	74.6	19.3	46.1	26.3
DiffSeg [15]	✗	76.0	21.2	72.5	43.6
iSeg (Ours)	✗	78.7	25.0	74.5	45.2

Mask generation on synthetic dataset. Fig. 5 presents some qualitative results of our proposed iSeg and DiffuMask [18]. The synthetic images are from DiffuMask [18]. DiffuMask first generates coarse pseudo masks using cross-attention map, and then train an AffinityNet to generate more precise pseudo masks. Compared to DiffuMask, our proposed iSeg has more accurate segmentation results without using any training processing. More results on synthetic images can be found in appendix C.

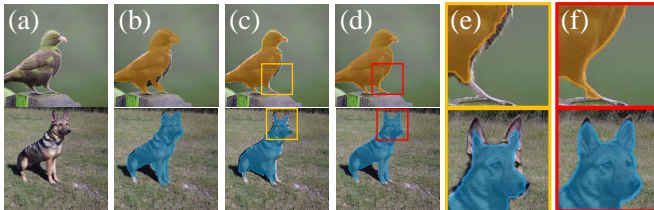


Figure 5: **Mask generation on synthetic dataset.** For synthetic image (a), DiffuMask first generates coarse pseudo mask using cross-attention map (b) and refines it with AffinityNet (c). Instead of using AffinityNet, we employ our method to refine cross-attention map (d). Our method can generate more accurate masks for these synthetic images, zoomed in (e,f).

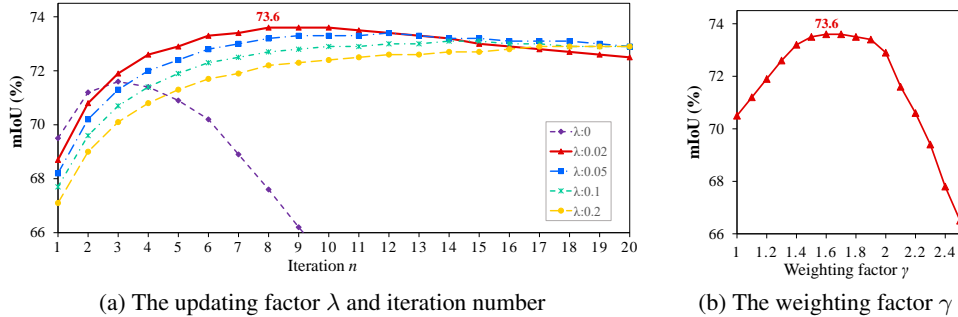


Figure 6: **Hyper-parameter study.** In (a), we show the impact of the updating factor λ in Ent-Self and the number n of iterations. When $\lambda = 0.02$ and $n = 8$, it has the best performance. In (b), we present the impact of the weighting factor γ in Cat-Cross. When $\gamma = 1.6$, it has the best performance.

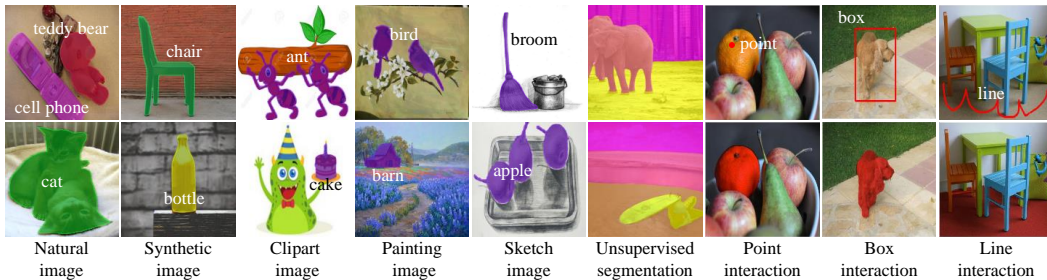


Figure 7: **Segmentation visualization** on various kinds of images and interactions.

4.2 Ablation study

Impact of integrating two proposed modules. Table 4 shows the results on PASCAL VOC training set. When integrating entropy-reduced self-attention (Ent-Self) module, it achieves a performance improvement of 4.1%. When integrating category-enhanced cross-attention (Cat-Cross) module, it presents a performance improvement of 2.9%. By integrating both Ent-Self and Cat-Cross into the baseline, it totally improves the baseline by 7.6%, which demonstrates that two proposed modules are complementary. Specifically, Cat-Cross module provides a better input for refinement, while Ent-Self module avoids the performance degradation during refinement.

Table 4: **Impact of the two modules.** We evaluate on PASCAL VOC training set. Our results are means of 10 seeds $\pm \delta$.

Ent-Self	Cat-Cross	mIoU
✗	✗	66.0 ± 0.3
✓	✗	70.1 ± 0.4
✗	✓	68.9 ± 0.2
✓	✓	73.6 ± 0.3

Hyper-parameter settings. There are some hyper-parameters in our method, including the updating factor λ in our Ent-Self module, the number of iterations N , and the weighting factor γ in our Cat-Cross module. Fig. 6(a) presents the impact of λ and N . When $\lambda = 0$ (namely using original self-attention map), iterative refinement presents a fast performance drop after several iterations. With a relatively large λ (e.g., 0.05), iterative refinement initially improves performance, and then keeps relatively stable performance. When $\lambda = 0.02$ and $N = 8$, it achieves best performance. Fig. 6(b) presents the impact of weighting factor γ . Increasing γ initially leads to improved performance but eventually results in performance drop. The best performance is achieved when $\gamma = 1.6$.

4.3 Segmentation with different kinds of images and interactions

Fig. 7 shows that our method supports segmentation on different kinds of images and interactions. At left, our method performs accurate segmentation of given categories on natural, synthetic, clipart, painting and sketch images. At right, our method can support different interactions to perform segmentation, where the initial segmentation map is generated by unsupervised segmentation maps, point, box, and line, and then fed to our iterative refinement with Self-Ent module. More results are in Appendix C. We also provide a video demo in supplementary material.

5 Conclusion

In this paper, we propose an iterative refinement framework for training-free segmentation using pre-trained stable diffusion model, named iSeg. Our proposed iSeg introduces two novel modules: entropy-reduced self-attention module and category-enhanced cross-attention module. The entropy-reduced self-attention module aims to suppress irrelevant global information within self-attention map, while the category-enhanced cross-attention module pays more attention to the features of given segmented categories. With these two proposed modules, our proposed method can generate accurate segmentation masks without any training on segmentation datasets. We perform the experiments on various datasets and segmentation tasks to demonstrate the efficacy of our proposed method.

Limitations and future work. Currently, we set the number of iterations in our iterative refinement as a fixed number, which is not optimal. In fact, the number of iterations can be dynamically changed according to the image. In future, we will explore image-aware iterative refinement framework.

References

- [1] Liang-Chieh Chen, George Papandreou, Florian Schroff, and et al. Rethinking atrous convolution for semantic image segmentation. *arXiv preprint arXiv:1706.05587*, 2017.
- [2] Huiyu Wang, Yukun Zhu, Hartwig Adam, and et al. Max-deeplab: End-to-end panoptic segmentation with mask transformers. In *IEEE/CVF Conference on Computer Vision and Pattern Recognition*, pages 5459–5470, 2021.
- [3] Enze Xie, Wenhai Wang, Zhiding Yu, and et al. SegFormer: Simple and efficient design for semantic segmentation with transformers. In *Conference on Neural Information Processing Systems*, pages 12077–12090, 2021.
- [4] Hubert Lin, Paul Upchurch, and Kavita Bala. Block annotation: Better image annotation with sub-image decomposition. In *IEEE/CVF International Conference on Computer Vision*, pages 5289–5299, 2019.
- [5] Alec Radford, Jong Wook Kim, Chris Hallacy, and et al. Learning transferable visual models from natural language supervision. In *International Conference on Machine Learning*, pages 8748–8763, 2021.
- [6] Feng Liang, Bichen Wu, Xiaoliang Dai, and et al. Open-vocabulary semantic segmentation with mask-adapted clip. In *IEEE/CVF Conference on Computer Vision and Pattern Recognition*, pages 7061–7070, 2023.
- [7] Yuqi Lin, Minghao Chen, Wenxiao Wang, and et al. CLIP is also an efficient segmenter: A text-driven approach for weakly supervised semantic segmentation. In *IEEE/CVF Conference on Computer Vision and Pattern Recognition*, pages 15305–15314, 2023.
- [8] Jiarui Xu, Shalini De Mello, Sifei Liu, and et al. GroupViT: Semantic segmentation emerges from text supervision. In *IEEE/CVF Conference on Computer Vision and Pattern Recognition*, pages 18134–18144, 2022.
- [9] Jinheng Xie, Xianxu Hou, Kai Ye, and et al. Clims: Cross language image matching for weakly supervised semantic segmentation. In *IEEE/CVF Conference on Computer Vision and Pattern Recognition*, pages 4483–4492, 2022.
- [10] Robin Rombach, Andreas Blattmann, Dominik Lorenz, and et al. High-resolution image synthesis with latent diffusion models. In *IEEE/CVF Conference on Computer Vision and Pattern Recognition*, pages 10674–10685, 2022.
- [11] Julia Wolleb, Robin Sandkühler, Florentin Bieder, and et al. Diffusion models for implicit image segmentation ensembles. In *International Conference on Medical Imaging with Deep Learning*, pages 1336–1348, 2022.
- [12] Dmitry Baranchuk, Ivan Baranchuk, Andrey Voynov, and et al. Label-efficient semantic segmentation with diffusion models. In *International Conference on Learning Representations*, 2022.
- [13] Wenliang Zhao, Yongming Rao, Zuyan Liu, and et al. Unleashing text-to-image diffusion models for visual perception. In *IEEE/CVF International Conference on Computer Vision*, pages 5706–5716, 2023.
- [14] Qiang Wan, Zilong Huang, Bingyi Kang, and et al. Harnessing diffusion models for visual perception with meta prompts. *arXiv preprint arXiv:2312.14733*, 2023.

- [15] Junjiao Tian, Lavisha Aggarwal, Andrea Colaco, and et al. Diffuse, attend, and segment: Unsupervised zero-shot segmentation using stable diffusion. *arXiv preprint arXiv:2308.12469*, 2023.
- [16] Jinglong Wang, Xiawei Li, Jing Zhang, and et al. Diffusion model is secretly a training-free open vocabulary semantic segmenter. *arXiv preprint arXiv:2309.02773*, 2023.
- [17] Changming Xiao, Qi Yang, Zhou Feng, and et al. From text to mask: Localizing entities using the attention of text-to-image diffusion models. *arXiv preprint arXiv:2309.04109*, 2023.
- [18] Weijia Wu, Yuzhong Zhao, Mike Zheng Shou, and et al. DiffuMask: Synthesizing images with pixel-level annotations for semantic segmentation using diffusion models. In *IEEE/CVF International Conference on Computer Vision*, pages 1206–1217, 2023.
- [19] Jonathan Long, Evan Shelhamer, and Trevor Darrell. Fully convolutional networks for semantic segmentation. In *IEEE/CVF Conference on Computer Vision and Pattern Recognition*, pages 431–440, 2015.
- [20] Liang-Chieh Chen, George Papandreou, Iasonas Kokkinos, and et al. DeepLab: Semantic image segmentation with deep convolutional nets, atrous convolution, and fully connected CRFs. *IEEE Transactions on Pattern Analysis and Machine Intelligence*, 40:834–848, 2018.
- [21] Wei Liu, Dragomir Anguelov, Dumitru Erhan, and et al. SSD: Single shot multibox detector. In *European Conference on Computer Vision*, pages 21–37, 2016.
- [22] Vijay Badrinarayanan, Alex Kendall, and Roberto Cipolla. SegNet: A deep convolutional encoder-decoder architecture for image segmentation. *IEEE Transactions on Pattern Analysis and Machine Intelligence*, 39:2481–2495, 2017.
- [23] Liang-Chieh Chen, Yukun Zhu, George Papandreou, and et al. Encoder-decoder with atrous separable convolution for semantic image segmentation. In *European Conference on Computer Vision*, pages 801–818, 2018.
- [24] Jun Fu, Jing Liu, Haijie Tian, and et al. Dual attention network for scene segmentation. In *IEEE/CVF Conference on Computer Vision and Pattern Recognition*, pages 3141–3149, 2019.
- [25] Zilong Huang, Xinggang Wang, Lichao Huang, and et al. CCNet: Criss-cross attention for semantic segmentation. In *IEEE/CVF International Conference on Computer Vision*, pages 603–612, 2019.
- [26] Yuhui Yuan, Lang Huang, Jianyuan Guo, and et al. OCNet: Object context for semantic segmentation. *International Journal of Computer Vision*, 129:2375–2398, 2021.
- [27] Alexey Dosovitskiy, Lucas Beyer, Alexander Kolesnikov, and et al. An image is worth 16x16 words: Transformers for image recognition at scale. In *International Conference on Learning Representations*, 2021.
- [28] Nicolas Carion, Francisco Massa, Gabriel Synnaeve, and et al. End-to-end object detection with transformers. In *European Conference on Computer Vision*, pages 213–229, 2020.
- [29] Yuhui Yuan, Rao Fu, Lang Huang, and et al. HRFormer: High-resolution transformer for dense prediction. In *Conference on Neural Information Processing Systems*, pages 7281–7293, 2021.
- [30] Jiaqi Gu, Hyoukjun Kwon, Dilin Wang, and et al. Multi-scale high-resolution vision transformer for semantic segmentation. In *IEEE/CVF Conference on Computer Vision and Pattern Recognition*, pages 12084–12093, 2022.
- [31] Bowen Cheng, Alex Schwing, and Alexander Kirillov. Per-pixel classification is not all you need for semantic segmentation. In *Conference on Neural Information Processing Systems*, volume 34, pages 17864–17875, 2021.
- [32] Bowen Cheng, Ishan Misra, Alexander G Schwing, and et al. Masked-attention mask transformer for universal image segmentation. In *IEEE/CVF Conference on Computer Vision and Pattern Recognition*, pages 1290–1299, 2022.
- [33] George Papandreou, Liang-Chieh Chen, Kevin P Murphy, and et al. Weakly-and semi-supervised learning of a deep convolutional network for semantic image segmentation. In *IEEE International Conference on Computer Vision*, pages 1742–1750, 2015.
- [34] Pedro O Pinheiro and Ronan Collobert. From image-level to pixel-level labeling with convolutional networks. In *IEEE/CVF Conference on Computer Vision and Pattern Recognition*, pages 1713–1721, 2015.

- [35] Jiwoon Ahn and Suha Kwak. Learning pixel-level semantic affinity with image-level supervision for weakly supervised semantic segmentation. In *IEEE/CVF Conference on Computer Vision and Pattern Recognition*, pages 4981–4990, 2018.
- [36] Bolei Zhou, Aditya Khosla, Agata Lapedriza, and et al. Learning deep features for discriminative localization. In *IEEE/CVF Conference on Computer Vision and Pattern Recognition*, pages 2921–2929, 2016.
- [37] Boyi Li, Kilian Q Weinberger, Serge Belongie, and et al. Language-driven semantic segmentation. In *International Conference on Learning Representations*, 2022.
- [38] Golnaz Ghiasi, Xiuye Gu, Yin Cui, and Tsung-Yi Lin. Scaling open-vocabulary image segmentation with image-level labels. In *European Conference on Computer Vision*, pages 540–557, 2022.
- [39] Xu Ji, João Henriques, and Andrea Vedaldi. Invariant information clustering for unsupervised image classification and segmentation. In *IEEE/CVF International Conference on Computer Vision*, pages 9864–9873, 2019.
- [40] Hamilton Mark, Zhang Zhoutong, Hariharan Bharath, and et al. Unsupervised semantic segmentation by distilling feature correspondences. In *International Conference on Learning Representations*, 2022.
- [41] Gyungin Shin, Weidi Xie, and Samuel Albanie. ReCo: Retrieve and co-segment for zero-shot transfer. In *Conference on Neural Information Processing Systems*, 2022.
- [42] Prafulla Dhariwal and Alexander Nichol. Diffusion models beat gans on image synthesis. In *Conference on Neural Information Processing Systems*, pages 8780–8794, 2021.
- [43] Neehar Kondapaneni, Markus Marks, Manuel Knott, and et al. Text-image alignment for diffusion-based perception. *arXiv preprint arXiv:2310.00031*, 2023.
- [44] Aliasghar Khani, Saeid Asgari Taghanaki, Aditya Sanghi, and et al. SLiMe: Segment like me. *arXiv preprint arXiv:2309.03179*, 2023.
- [45] Yuanfeng Ji, Zhe Chen, Enze Xie, and et al. DDP: Diffusion model for dense visual prediction. In *IEEE/CVF International Conference on Computer Vision*, pages 21684–21695, 2023.
- [46] Laurynas Karazija, Iro Laina, Andrea Vedaldi, and et al. Diffusion models for zero-shot open-vocabulary segmentation. *arXiv preprint arXiv:2306.09316*, 2023.
- [47] Junnan Li, Dongxu Li, Caiming Xiong, and et al. BLIP: Bootstrapping language-image pre-training for unified vision-language understanding and generation. In *International Conference on Machine Learning*, pages 12888–12900, 2022.
- [48] Aditya Ramesh, Prafulla Dhariwal, Alex Nichol, and et al. Hierarchical text-conditional image generation with clip latents. *arXiv preprint arXiv:2204.06125*, 2022.
- [49] Alex Nichol, Prafulla Dhariwal, Aditya Ramesh, and et al. GLIDE: Towards photorealistic image generation and editing with text-guided diffusion models. In *International Conference on Machine Learning*, pages 16784–16804, 2022.
- [50] Chitwan Saharia, William Chan, Saurabh Saxena, and et al. Photorealistic text-to-image diffusion models with deep language understanding. In *Conference on Neural Information Processing Systems*, pages 36479–36494, 2022.
- [51] Christoph Schuhmann, Romain Beaumont, Richard Vencu, and et al. Laion-5B: An open large-scale dataset for training next generation image-text models. In *Conference on Neural Information Processing Systems*, volume 35, pages 25278–25294, 2022.
- [52] Diederik P Kingma and Max Welling. Auto-encoding variational bayes. In *International Conference on Learning Representations*, 2014.
- [53] Olaf Ronneberger, Philipp Fischer, and Thomas Brox. U-net: Convolutional networks for biomedical image segmentation. In *International Conference on Medical Image Computing and Computer-Assisted Intervention*, pages 234–241, 2015.
- [54] Zhiyu Jin, Xuli Shen, Bin Li, and et al. Training-free diffusion model adaptation for variable-sized text-to-image synthesis. In *Conference on Neural Information Processing Systems*, volume 36, 2023.

- [55] Jiwoon Ahn, Sunghyun Cho, and Suha Kwak. Weakly supervised learning of instance segmentation with inter-pixel relations. In *IEEE/CVF Conference on Computer Vision and Pattern Recognition*, pages 2209–2218, 2019.
- [56] Jungbeom Lee, Eunji Kim, and Sungroh Yoon. Anti-adversarially manipulated attributions for weakly and semi-supervised semantic segmentation. In *IEEE/CVF Conference on Computer Vision and Pattern Recognition*, pages 4071–4080, 2021.
- [57] Wei Zhai, Pingyu Wu, Kai Zhu, and et al. Background activation suppression for weakly supervised object localization and semantic segmentation. *International Journal of Computer Vision*, 132(3):750–775, 2024.
- [58] Yuanchen Wu, Xiaoqiang Li, Songmin Dai, and et al. Hierarchical semantic contrast for weakly supervised semantic segmentation. In *International Joint Conference on Artificial Intelligence*, pages 1542–1550, 2023.
- [59] Lian Xu, Wanli Ouyang, Mohammed Bennamoun, and et al. Multi-class token transformer for weakly supervised semantic segmentation. In *IEEE/CVF Conference on Computer Vision and Pattern Recognition*, pages 4310–4319, 2022.
- [60] Lian Xu, Mohammed Bennamoun, Farid Boussaid, and et al. MCTFormer+: Multi-class token transformer for weakly supervised semantic segmentation. *arXiv preprint arXiv:2308.03005*, 2023.
- [61] Lixiang Ru, Heliang Zheng, Yibing Zhan, and et al. Token contrast for weakly-supervised semantic segmentation. In *IEEE/CVF Conference on Computer Vision and Pattern Recognition*, pages 3093–3102, 2023.
- [62] Lianghui Zhu, Yingyue Li, Jiemin Fang, and et al. WeakTr: Exploring plain vision transformer for weakly-supervised semantic segmentation. *arXiv preprint arXiv:2304.01184*, 2023.
- [63] Chong Zhou, Chen Change Loy, and Bo Dai. Extract free dense labels from clip. In *European Conference on Computer Vision*, pages 696–712, 2022.
- [64] Huaishao Luo, Junwei Bao, Youzheng Wu, and et al. SegCLIP: Patch aggregation with learnable centers for open-vocabulary semantic segmentation. In *International Conference on Machine Learning*, pages 23033–23044, 2023.
- [65] Kanchana Ranasinghe, Brandon McKinzie, Sachin Ravi, and et al. Perceptual grouping in contrastive vision-language models. In *IEEE/CVF International Conference on Computer Vision*, pages 5548–5561, 2023.
- [66] Pengzhen Ren, Changlin Li, Hang Xu, and et al. ViewCo: Discovering text-supervised segmentation masks via multi-view semantic consistency. *arXiv preprint arXiv:2302.10307*, 2023.
- [67] Yuqi Lin, Minghao Chen, Kaipeng Zhang, and et al. TagCLIP: A local-to-global framework to enhance open-vocabulary multi-label classification of clip without training. In *AAAI Conference on Artificial Intelligence*, pages 3513–3521, 2024.
- [68] Mark Everingham, Luc Van Gool, Christopher KI Williams, and et al. The pascal visual object classes (voc) challenge. *International Journal of Computer Vision*, 88:303–338, 2010.
- [69] Tsung-Yi Lin, Michael Maire, Serge Belongie, and et al. Microsoft COCO: Common objects in context. In *European Conference on Computer Vision*, pages 740–755, 2014.
- [70] Roozbeh Mottaghi, Xianjie Chen, Xiaobai Liu, and et al. The role of context for object detection and semantic segmentation in the wild. In *IEEE Conference on Computer Vision and Pattern Recognition*, pages 891–898, 2014.
- [71] Mathilde Caron, Piotr Bojanowski, Armand Joulin, and et al. Deep clustering for unsupervised learning of visual features. In *European Conference on Computer Vision*, pages 139–156, 2018.
- [72] Jang Hyun Cho, Utkarsh Mall, Kavita Bala, and et al. PICIE: Unsupervised semantic segmentation using invariance and equivariance in clustering. In *IEEE/CVF Conference on Computer Vision and Pattern Recognition*, pages 16789–16799, 2021.
- [73] Marius Cordts, Mohamed Omran, Sebastian Ramos, and et al. The cityscapes dataset for semantic urban scene understanding. In *IEEE/CVF Conference on Computer Vision and Pattern Recognition*, pages 3213–3223, 2016.

- [74] Holger Caesar, Jasper Uijlings, and Vittorio Ferrari. COCO-Stuff: Thing and stuff classes in context. In *IEEE/CVF Conference on Computer Vision and Pattern Recognition*, pages 1209–1218, 2018.
- [75] Xingchao Peng, Qinxun Bai, Xide Xia, Zijun Huang, Kate Saenko, and Bo Wang. Moment matching for multi-source domain adaptation. In *IEEE/CVF International Conference on Computer Vision*, pages 1406–1415, 2019.

A Algorithms

Algorithm 1 presents the pseudo code about how to refine the cross-attention by entropy-reduced self-attention iteratively using our proposed iSeg.

Algorithm 1 Pipeline of our proposed iSeg

- 1: **Input:**
 - 2: γ : weighting factor of Cat-Cross Module;
 - 3: λ : updating factor of Ent-Self Module;
 - 4: N : iteration number; i : category index;
 - 5: **Output:**
 - 6: M_p : predicted segmentation mask.
 - 7: Generate latent features z and text embeddings ε of the image and text prompt, respectively.
 - 8: Compute category-enhanced text embeddings $\varepsilon_{en} \leftarrow \text{Cat-Cross}(\varepsilon, i, \gamma)$
 - 9: Extract and select A_{sa} and A_{ca} from denoising UNet
 - 10: Compute entropy-reduced self-attention $A_{sa}^{ent} \leftarrow \text{Ent-Self}(A_{sa}, \lambda)$
 - 11: Set $n = 1$ and $A_{ca}^0 = A_{ca}$
 - 12: **repeat**
 - 13: Normalize the cross-attention map A_{ca}^{n-1}
 - 14: Update the refined cross-attention map $A_{ca}^n \leftarrow A_{sa}^{ent} * A_{ca}^{n-1}$
 - 15: Update $n \leftarrow n + 1$
 - 16: **until** n is larger than N
 - 17: Normalize the refined cross-attention map A_{ca}^N
 - 18: Generate the segmenation mask $M_p \leftarrow A_{ca}^N[i]$ at index i of text prompt
 - 19: **return** M_p
-

B More implementation details

Here we present more implementation details of our proposed method on different segmentation tasks, including weakly-supervised semantic segmentation, open-vocabulary semantic segmentation, unsupervised segmentation, and mask generation for synthetic dataset.

Weakly-supervised semantic segmentation. In weakly-supervised semantic segmentation, one of the key is to generate pseudo pixel-level masks for training set. We compare our training-free method with existing approaches for pixel-level mask generation on two datasets, including PASCAL VOC 2012 [68] and MS COCO 2014 [69]. Specifically, we use the categories existing in image to generate a template such as ‘A photograph of [CLS A] and [CLS B] and other objects and background’. Here we compose the sentence with some general words, such as ‘object’ and ‘background’ rather than specific background category associated with the specific dataset similar to CLIPES [7].

Open-vocabulary semantic segmentation. Open-vocabulary semantic segmentation aims to perform segmentation of arbitrary categories. We compare our training-free method with existing approaches on three datasets, including PASCAL VOC 2012 (VOC), PASCAL-Context (Context), and MS COCO Object (Object). To perform open-vocabulary semantic segmentation, we employ the pre-trained CLIP to generate image-level labels as text prompts following TagCLIP [67]. Afterwards, we keep the same settings as weakly-supervised semantic segmentation task to obtain the final mask.

Unsupervised segmentation. We compare our training-free method with other unsupervised segmentation approaches on two datasets, including COCO-Stuff-27 [74] and Cityscapes [73]. We integrate our proposed method into the training-free approach DiffSeg [15] as a post-processing. Specifically, we treat the segmentation results of DiffSeg as initial cross-attention maps, and employ our proposed

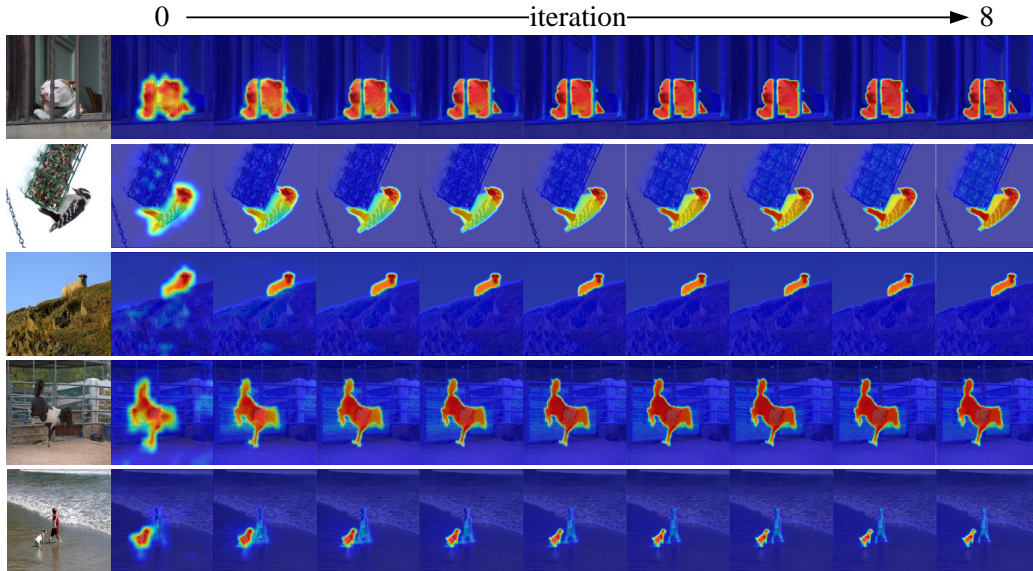


Figure 8: **Refined cross-attention maps** of our proposed iSeg at different iterations.



Figure 9: **Segmentation results** on synthetic images.

entropy-reduced self-attention module to perform iterative refinement, while the other settings are consistent with DiffSeg.

Mask generation for synthetic dataset. Recently, some researchers have explored generating synthetic dataset for semantic segmentation. In this task, it is important to generate the mask labels for synthetic images. DiffuMask [18] utilizes cross-attention maps in diffusion model to generate pseudo masks for synthetic images, which are further refined by AffinityNet. Here, we can directly apply our iterative refinement to improve the initial pseudo masks generated by DiffuMask on synthetic dataset without requiring any additional refinements like AffinityNet.

C Qualitative results

Cross-attention map after different iterations. Fig. 8 visualizes some refined cross-attention maps of our proposed iSeg at different refinement iterations. With the increment of iterations ranging from 0 to 8, our proposed iSeg can generate more accurate cross-attention maps of corresponding objects.



Figure 10: Segmentation results on PASCAL VOC 2012 and MS COCO 2014 datasets.

Results on synthetic images. Fig. 9 presents some segmentation results of our proposed iSeg on synthetic images generated by DiffuMask [18]. It can be observed that our proposed method can generate accurate segmentation masks for diverse synthetic images.

Results on natural images. Fig. 10 presents some segmentation results of our proposed iSeg on PASCAL VOC 2012 and MS COCO. It can be observed that our proposed method can generate accurate segmentation masks for various categories.

Results of unsupervised segmentation. Fig. 11 presents some unsupervised segmentation results of our proposed iSeg on COCO-Stuff-27 datasets. Our proposed method is able to accurately group the pixels into different objects.

Cross-domain results. Fig. 12 presents some kind of image segmentation on DomainNet [75]. Our proposed method is able to accurately segment different kinds of objects including sketch, painting and clipart according to given category.

Results using different interactions. Fig. 13 presents more segmentation results using different interactions, such as points, lines, and boxes.

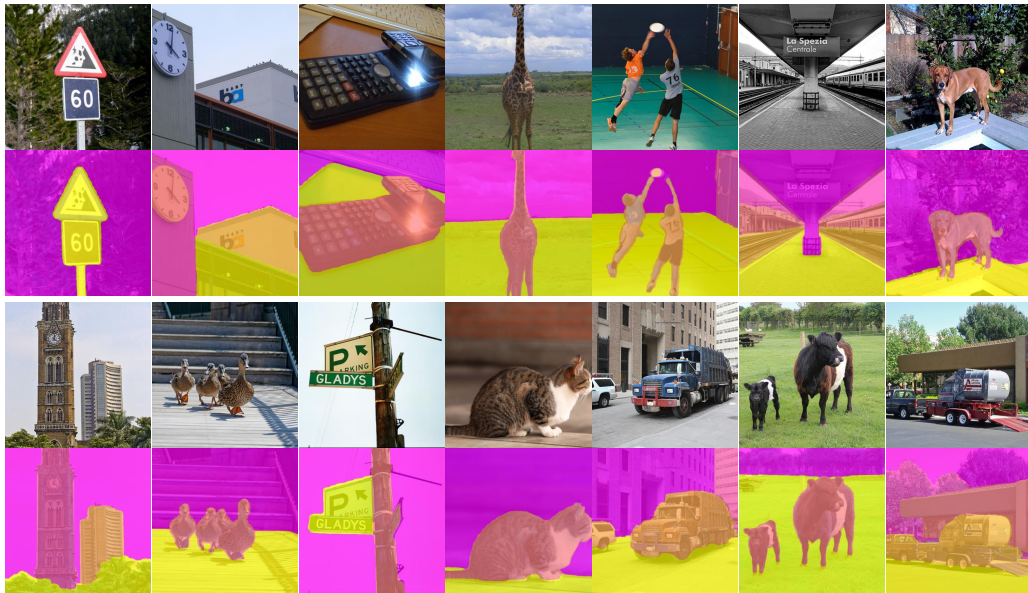


Figure 11: **Unsupervised segmentation results** on COCO-Stuff-27 dataset.

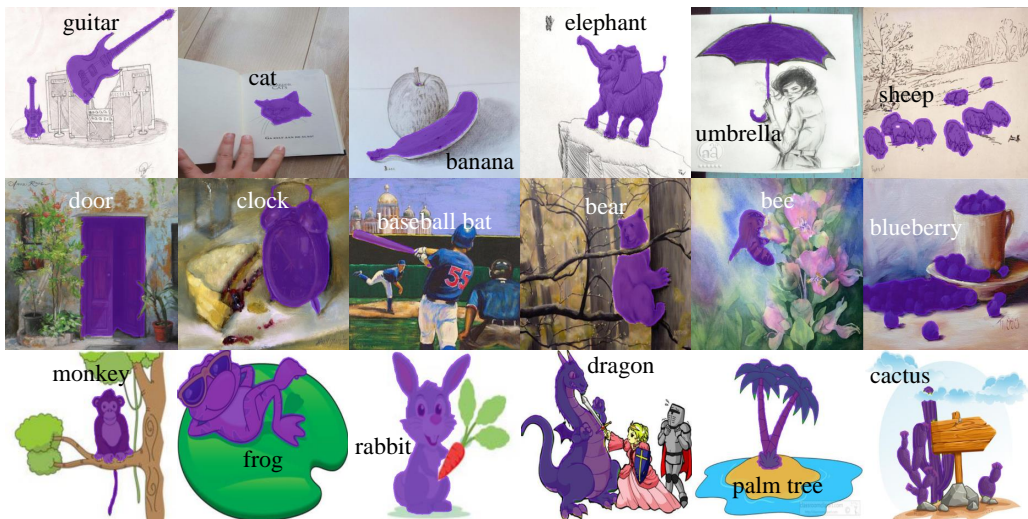
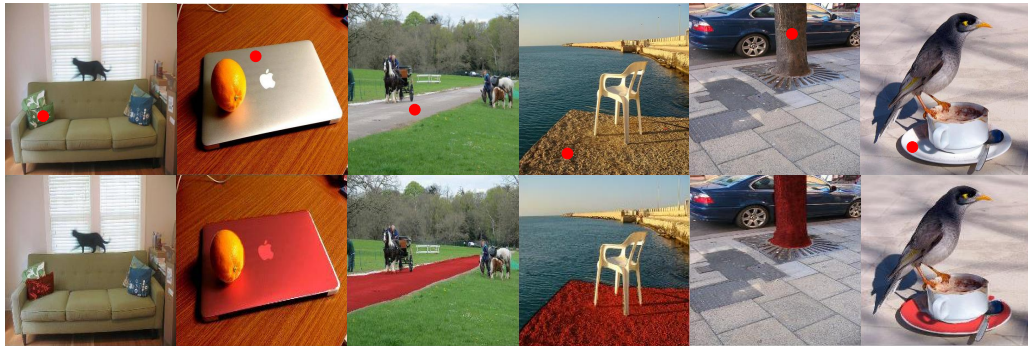
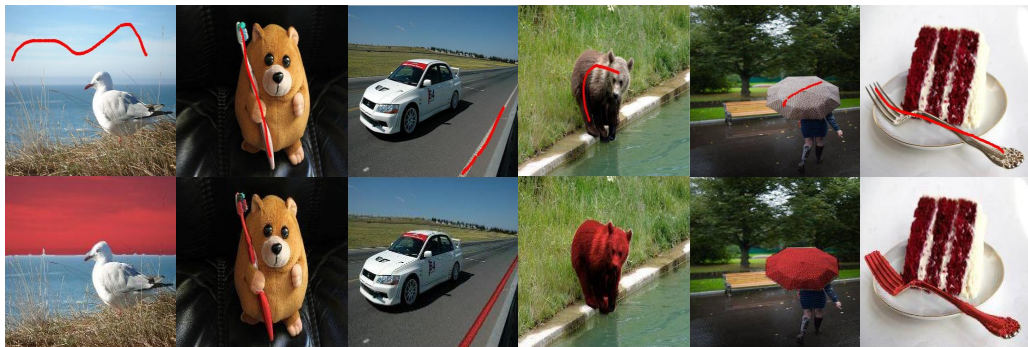


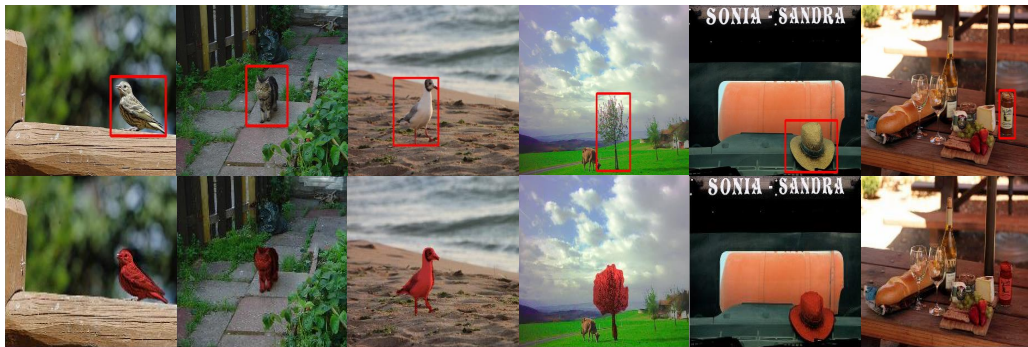
Figure 12: **Cross-domain segmentation results** on DomainNet Sketch part (top), DomainNet Painting part (middle), DomainNet Clipart part (bottom).



(a) Point interaction



(b) Line interaction



(c) Box interaction

Figure 13: Segmentation results using different interactions, including points, boxes, and lines.